

NUMERICAL MODELING OF DAMPER CONFIGURATION AND  
ARRANGEMENTS FOR ANALYSING THERMAL STRATIFICATION IN  
MODULAR AIR HANDLING UNITS

By

ROHIT ANTONY RAYMONDS

Presented to the Faculty of the Graduate School of  
The University of Texas at Arlington in Partial Fulfillment  
of the Requirements for the Degree of

MASTER OF SCIENCE IN MECHANICAL ENGINEERING

THE UNIVERSITY OF TEXAS AT ARLINGTON

MAY 2023

Copyright by  
Rohit Antony Raymonds  
2023

## ACKNOWLEDGEMENT

I would like to take this opportunity to express my heartfelt appreciation to everyone who contributed to the success of my research project. First and foremost, I must extend my sincere gratitude to my thesis advisor, **Dr. Dereje Agonafer**, whose guidance, support, and valuable suggestions were instrumental in shaping my research and enabling me to achieve my goals. Dr. Agonafer's expertise and mentorship were crucial in helping me navigate the challenges and complexities of this project.

In addition, I am deeply grateful to my committee members, **Dr. Rajesh Kasukurthy** and **Dr. Adolhossein Haji Sheik**, for their valuable feedback and insightful suggestions. Their contributions helped me to improve the quality of my research and made my work more impactful.

I would also in debt to thank my colleagues, **Vibin Shalom, Anto Joseph Barigala Charles Paulraj, and Akiileesh Sivakumar**, for their unwavering support and assistance throughout this project. Their encouragement and guidance were instrumental in keeping me motivated and focused on achieving my objectives.

Furthermore, I am grateful to my **EMNSPC** team for their collaboration, cooperation, and encouragement. Their teamwork and support helped me to overcome various obstacles and complete this project successfully.

Finally, I must express my heartfelt gratitude to my parents, Mr. Xavier Francis Raymonds and Mrs. J. Merry Geisa, for their support, and sacrifices. Their financial and emotional assistance played a significant role in enabling me to pursue my dreams and reach this level of success.

In conclusion, I would like to acknowledge and thank God Almighty for providing me with the strength, courage, and determination to pursue my goals with passion and perseverance. I am truly grateful to everyone who contributed to this project, and I look forward to continuing my research with renewed enthusiasm and commitment.

## ABSTRACT

### NUMERICAL MODELING OF DAMPER CONFIGURATION AND ARRANGEMENTS FOR ANALYSING THERMAL STRATIFICATION IN MODULAR AIR HANDLING UNITS

Rohit Antony Raymonds

The University of Texas at Arlington, 2023

Advisor: Dr. Dereje Agonafer

Although air handling units are well established and matured there are opportunities to optimize and improve the overall thermal and flow performance to reduce the carbon footprint of an air-cooled data center. Airside economization (ASE) arrangement to use cold outdoor air to minimize mechanical cooling energy was substantial progress in minimizing the power usage effectiveness (PUE) for data centers. ASE is an arrangement of ducts and dampers with the necessary controls to meet the cooling requirements. Dampers play a significant role in regulating the mass flow rate of the air and in mixing the two air streams: cold outdoor air, and hot return air from the data center to a precondition. The effective mixing of these two air streams is of at most importance to minimize the stratification and improve the performance of the subsequent air conditioning processes such as direct/indirect evaporative cooling. Existing literature investigated the effects of different damper angles on the mixing effectiveness. But the literature lacks a comprehensive characterization and analysis of the damper sizing, configuration, and arrangement and its influence on the flow patterns and air stratification. The literature also lacks to encompass the effects of damper authority in properly matching the dampers to minimize the overall pressure drop. The objective of this article is to analyze the effect of different damper configurations (parallel/opposed blade), damper sizing, and damper matching on the mixing effectiveness of the air streams. A numerical model of dampers in an air handling unit (AHU) was validated using experimental data for the damper characteristics. Numerical modeling is used to parametrically iterate different damper configurations such as parallel flow, counter flow, and a combination of parallel and counter, damper angles. The pressure drop across the dampers and the mixing effectiveness were calculated to have a direct comparison between different damper designs and arrangements. It was observed that certain damper configurations and arrangements yielded higher mixing effectiveness. Opposed blade dampers performed better than parallel blade dampers when matched correctly. This study thereby provides a comprehensive guide for manufacturers to appropriately design AHU factoring in different parameters such as damper combinations and angles to provide optimum thermal and flow performance.

## LIST OF ABBREVIATIONS

P	Density (kg/m <sup>3</sup> )
k	Thermal Conductivity (W/m-K)
$\epsilon$	Kinematic Rate of Dissipation (m <sup>2</sup> /s <sup>3</sup> )
V	Velocity (m/s)
$\mu$	Viscosity (N/m <sup>2</sup> s)
m	Mass flow rate (kg/s)
q	Heat load (W)
P	Power (W)
v	Volumetric Flow Rate (cfm)
ASHRAE	American Society of Heating, Refrigeration and Air Conditioning Engineers
Re	Reynolds number
C <sub>p</sub>	Specific Heat capacity (J/kg K)
P	Pressure (in of H <sub>2</sub> O)
DEC	Direct Evaporative Cooling Unit
IEC	Indirect Evaporative Cooling Unit
OA	Outside air damper
RA	Return air damper

## LIST OF FIGURES

FIGURE		PAGE
1.	<i>Psychometric chart displaying various zones recommended by ASHRAE.....</i>	2
2.	<i>Table of ASHRAE recommendations for air cooled data.....</i>	2
3.	<i>Air side Economizer.....</i>	3
4.	<i>Direct Evaporative Cooling.....</i>	4
5.	<i>Indirect Evaporative Cooling.....</i>	4
6.	<i>Parallel Damper.....</i>	5
7.	<i>Schematic image of Parallel Damper.....</i>	5
8.	<i>Opposed Damper.....</i>	6
9.	<i>Schematic image of Opposed Damper.....</i>	6
10.	<i>Flow characteristics at different Damper Authorities.....</i>	7
11.	<i>Schematic image of Air flow bench.....</i>	8
12.	<i>Schematic image of front section of Air flow bench with Damper.....</i>	8
13.	<i>Image of Air Flow Bench.....</i>	9
14.	<i>Image of Front section of Air flow bench.....</i>	9
15.	<i>Image of Air flow bench with Flow sensors.....</i>	9
16.	<i>Plot for Pressure drop vs Flow rate.....</i>	10
17.	<i>CFD model for Air handling unit.....</i>	11
18.	<i>Adiabatic mixing schematic with process line on the psychrometric chart.....</i>	12

19.	<i>Adiabatic mixing of OA and RA on psychrometric chart.....</i>	<i>13</i>
20.	<i>Plot for Grid Sensitivity Analysis.....</i>	<i>14</i>
21.	<i>Table for Different Damper Combination.....</i>	<i>15</i>
22.	<i>Plot for Mixing Effectiveness and Total pressure drop vs different configurations for case 1 ...</i>	<i>16</i>
23.	<i>Plot for Mixing Effectiveness and Total pressure drop vs different configurations for case 2 ...</i>	<i>16</i>
24.	<i>Plot for Mixing Effectiveness and Total pressure drop vs different configurations for case 3....</i>	<i>17</i>
25.	<i>Plot for Mixing Effectiveness and Total pressure drop vs different configurations for case 4....</i>	<i>17</i>
26.	<i>Plot for Mixing Effectiveness and Total pressure drop vs different configurations for case 5 ...</i>	<i>18</i>
27.	<i>Plot for Mixing Effectiveness and Total pressure drop vs different configurations for case 6 ...</i>	<i>18</i>
28.	<i>Plot for Mixing Effectiveness Comparison.....</i>	<i>19</i>
29.	<i>Plot for Pressure drop Comparison.....</i>	<i>19</i>
30.	<i>Temperature Contour for Case 2.....</i>	<i>20</i>
31.	<i>Temperature Contour for Case 3.....</i>	<i>20</i>
32.	<i>Velocity Vectors for Case 2.....</i>	<i>20</i>
33.	<i>Velocity Vectors for Case 3.....</i>	<i>20</i>

# TABLE OF CONTENT

ACKNOWLEDGEMENT

ABSTRACT

LIST OF ABBREVIATIONS

LIST OF FIGURES

CHAPTER 1 – Introduction.....	01
CHAPTER 2 – Introduction to Free cooling and evaporative cooling .....	03
CHAPTER 3 – Introduction to Air handling units and dampers .....	05
CHAPTER 4 – Experimental Setup.....	08
CHAPTER 5 – CFD Modeling .....	11
CHAPTER 6 – Results and Discussion .....	15
CHAPTER 7 – Conclusion .....	22
REFERENCE.....	23

APPENDIX



## Chapter 1- Introduction

Data centers are crucial infrastructure facilities that house many servers and other computer equipment. These generally generate a significant amount of heat due to functions such as processing, management, storage and interchange of data and information. This leads to malfunction of the processors in use for which cooling systems are used to subside the temperature and run it in an optimum state. It became very crucial to run the Data center very efficiently in optimal space and resources and at the same time cost effectively. The cooling system occupies almost 30%-40% portion of the total energy consumption [1-16]. Traditional data centers globally have decreased their energy demand, from around 97.6 terawatt-hours in 2015, to some 50 terawatt-hours in 2019[17]. Cost reduction can be attained by using various techniques such as air side economization (ASE), Direct evaporative cooling (DEC) and Indirect evaporative cooling (IEC) and Direct Expansion Cooling.

According to a survey a PUE of 1.65 is considered as an ideal average for modern data centers. According to the [Uptime Institute's 2021 Data Center Survey](#), the global average of respondents' largest data centers is around 1.57 [18].

The American society of Heating, Refrigeration and Air Conditioning Engineers (ASHRAE) recommended few thermal guidelines for the safe operations of IT equipment in data centers. Prior to these guidelines, recommendations provided by the IT manufacturer on the operation of their product in data center environment, which were not accurate due to multiplicity of usage of equipment in a data center [19].

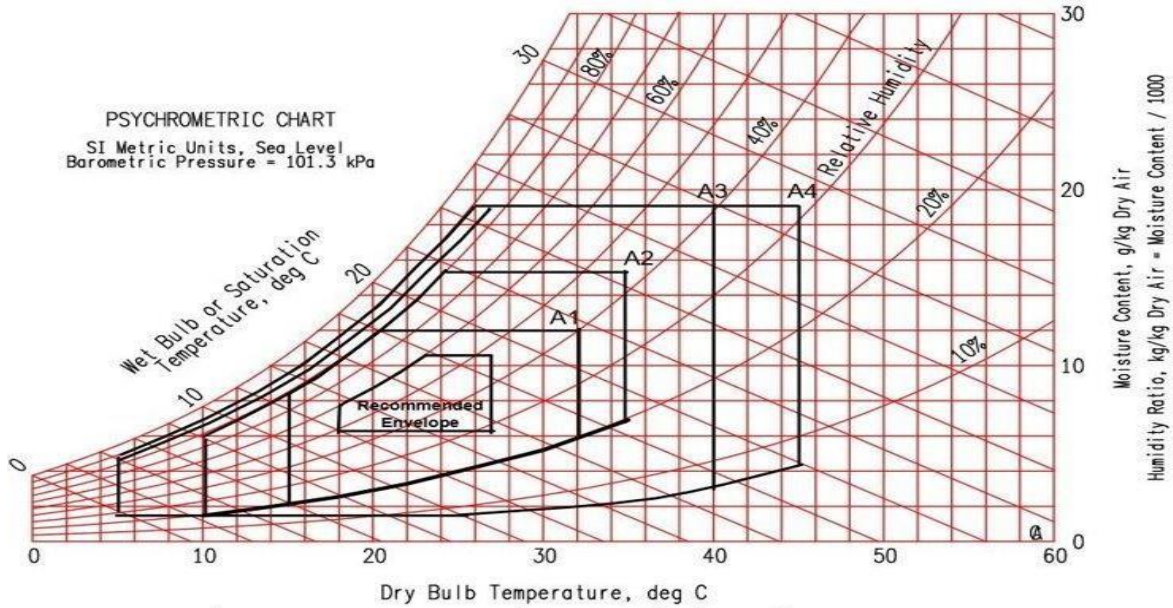


Figure 1- Psychrometric chart displaying various zones recommended by ASHRAE [19]

In 2011 ASHRAE released an updated thermal guideline for the data centers by publishing different classes.

Class <sup>a</sup>	Equipment Environmental Specifications for Air Cooling						
	Product Operations <sup>b,c</sup>					Product Power Off <sup>c,d</sup>	
	Dry-Bulb Temperature <sup>e,f</sup> °C	Humidity Range, Non-Condensing <sup>h,i,k,l</sup>	Maximum Dew Point <sup>k</sup> °C	Maximum Elevation <sup>e,j,m</sup> m	Maximum Temperature Change <sup>f</sup> in an Hour (°C)	Dry-Bulb Temperature °C	Relative Humidity <sup>h</sup> %
<b>Recommended (Suitable for all 4 classes)</b>							
A1 to A4	18 to 27	-9°C DP to 15°C DP and 60% RH					
<b>Allowable</b>							
A1	15 to 32	-12°C DP & 8% RH to 17°C DP and 80% RH <sup>k</sup>	17	3050	5/20	5 to 45	8 to 80
A2	10 to 35	-12°C DP & 8% RH to 21°C DP and 80% RH <sup>k</sup>	21	3050	5/20	5 to 45	8 to 80
A3	5 to 40	-12°C DP & 8% RH to 24°C DP and 85% RH <sup>k</sup>	24	3050	5/20	5 to 45	8 to 80
A4	5 to 45	-12°C DP & 8% RH to 24°C DP and 90% RH <sup>k</sup>	24	3050	5/20	5 to 45	8 to 80
B	5 to 35	8% to 28°C DP and 80% RH <sup>k</sup>	28	3050	NA	5 to 45	8 to 80
C	5 to 40	8% to 28°C DP and 80% RH <sup>k</sup>	28	3050	NA	5 to 45	8 to 80

Figure 2 - Table of ASHRAE recommendations for air cooled data [20]

## Chapter 2

### Introduction to Free cooling and evaporative cooling

#### **Air side economizer or free cooling:**

An air-side economizer is a device or mechanism that brings fresh outside air into a building's HVAC (heating, ventilation, and air conditioning) system, reducing the need for mechanical cooling. The air-side economizer takes advantage of cool outside air to provide free cooling and ventilation to a building, which can reduce energy consumption and costs associated with air conditioning. The system works by using sensors to monitor the temperature and humidity levels of the outside air and comparing them to the conditions inside the building. When the outside air is cooler and drier than the indoor air, the air-side economizer opens a damper to allow the outside air into the building, and the HVAC system shuts off the mechanical cooling. This process can also improve indoor air quality by flushing out stagnant air and introducing fresh air into the building. Air-side economizers can help reduce energy consumption and costs associated with cooling and ventilation, as well as improve indoor air quality and occupant comfort.

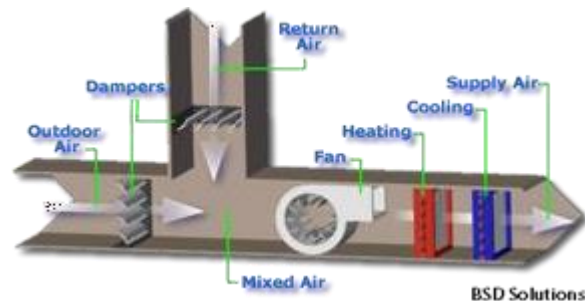


Figure 3 – Air side Economizer [21]

#### **Evaporative cooling**

Evaporative cooling is a natural process in which water absorbs heat from the surrounding air and evaporates, resulting in a cooling effect. The principle behind phase change cooling is that the use of warmth to vary from liquid to vapor [6]. Evaporative cooling techniques can be used where traditional cooling systems can be avoided. Evaporative cooling is more effective in dry climates where humidity is low because the air has a greater capacity to absorb water. Evaporative cooling is an energy-efficient alternative to traditional air conditioning systems, as it consumes significantly less energy. However, it may not be as effective in humid climates, as the air has less capacity to absorb water and the cooling effect is reduced. Additionally, it requires a steady supply of water and may increase humidity levels in the building or room.

## Types of Evaporative Cooling

There are two types of evaporative cooling systems, direct evaporative cooling, and indirect evaporative cooling.

### Direct Evaporative cooling

In direct evaporative cooling (DEC), the air from outside is introduced into water saturated medium and is cooled through evaporation. With the help of blower air is circulated inside the unit. DEC adds moisture to the air up to its saturation point. The dry bulb temperature is reduced keeping the wet bulb temperature constant. Most of the time these systems are used in home and industries. DEC is economical comparing it to vapor compression system also it consumes less energy [22].

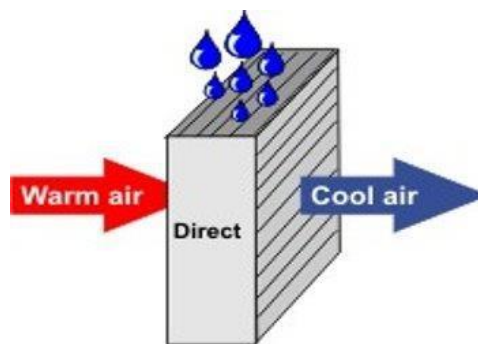


Figure 4 - Direct Evaporative Cooling [23]

### Indirect Evaporative cooling

In indirect evaporative cooling (IEC), a secondary air stream is cooled using water and is passed through a heat exchanger where it cools the primary air stream from the direct evaporative cooling method. This cooled air is circulated into a system using a blower. In this method moisture is not added to the primary air stream. Dry bulb and wet bulb temperatures are reduced [22].

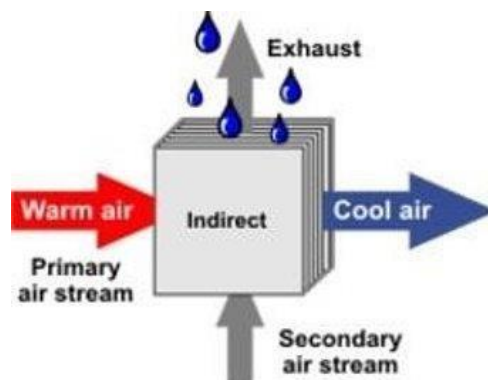


Figure 5 - Indirect Evaporative Cooling [23]

## Chapter 3

### Introduction to Air handling units and dampers

#### Air handling unit (AHU):

Modular air handling units (MAHUs) are commonly used in data center cooling and commercial buildings to regulate indoor air quality and temperature. The air handler is a large metal box connected to a duct, ventilation system that distributes the conditioned air throughout the building and returns to AHU. These units consist of several components, including dampers, filters, heating and cooling elements, humidifiers, mixing chambers which are critical to their operation. However, thermal stratification, which refers to the layering of air with different temperatures in a space, can occur within MAHUs due to poor damper configurations and arrangements. This can result in inefficient energy usage and poor indoor air quality.

#### Dampers:

A damper is a component that can regulate or completely block the flow of air in an HVAC mixing chamber. Air is usually supplied to the mixing chamber from different directions, and dampers, which can be controlled by a system, are responsible for controlling the airflow through the chamber. The airflow through an air outlet, inlet, or duct can be adjusted using dampers, which can be manually adjustable, or part of an automated control system.

#### Parallel Damper

Parallel blades rotate so they are always parallel to each other; therefore, at any partially open position, they tend to redirect airflow and increase turbulence and mixing within the downstream duct work or plenum. This characteristic makes them good candidates for return and outside air intake into a mixing chamber.



Figure 6- Parallel Damper

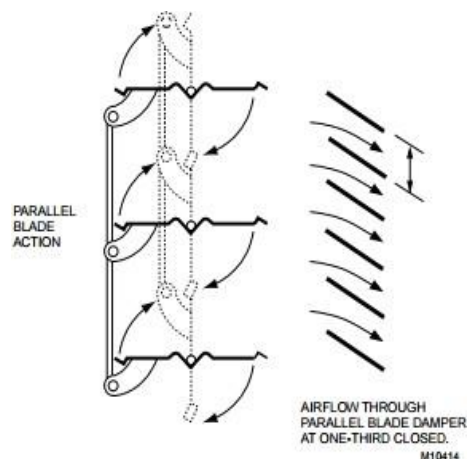


Figure 7- Schematic image of Parallel Damper [22]

## Opposed damper:

Opposed blades rotate opposite each other in adjacent pairs. Air discharge through this type of damper is straighter and a bit quieter under partial-flow conditions. Opposed blade dampers are often specified where air direction control is important relative to other factors, such as within final volume control devices. The flow characteristics of parallel and opposed dampers are different; an opposed blade damper must be opened further (creating a higher modulating pressure drop) to provide the same percentage of total air volume as a parallel damper (creating a lower modulating pressure drop). When they are wide open, the pressure drop is the same for both types.



Figure 8 - Opposed Damper

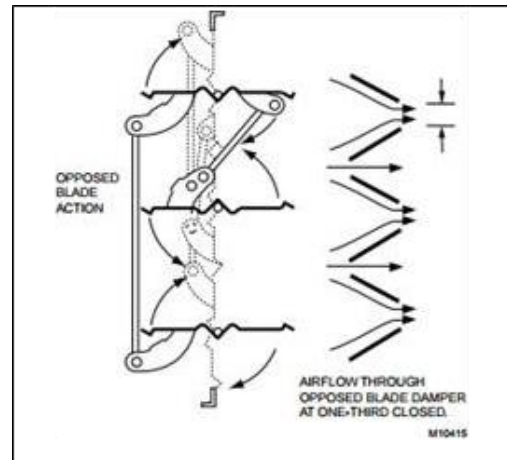


Figure 9 – Schematic image of Opposed Damper [22]

## Damper Authority:

Damper authority is crucial in correlating damper blade angles, velocity ratios and mixing volume ratios of OA and RA when utilizing motorized damper control and feedback configuration [9].

$$\text{Damper Authority (\%)} = \frac{(\text{Open Damper Resistance})}{(\text{Total System Resistance})} \times 100\%$$

At lower damper angle the flow increases at higher rate and Damper authority is minimum on the total pressure drop in the system. Based on the Damper Authority percentage, we can find the combination of the damper angle for the OA & RA.

To find the damper angle combination, we must calculate the percentage of the two-stream mixing. Once we know their respective percentages, we can calculate the damper angle from the flow characteristic curve using the damper authority.

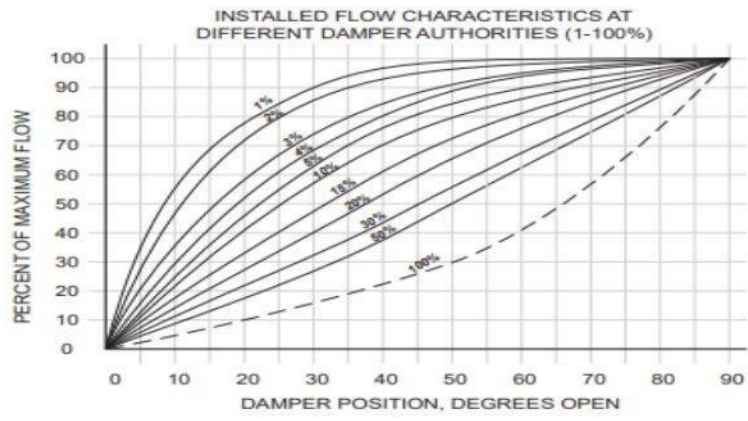


Fig 10- Flow characteristics at different Damper Authorities [23]

## Chapter 4

### Experimental setup

The experimental setup comprises of two chambers. A nozzle plate is positioned between these chambers, consisting of three 6-inch nozzles that can be opened or closed based on the experiment's requirements. The nozzle is selected based on our desired flow range. The chamber is constructed with pressure taps on each side of the nozzle to measure the pressure drop. The differential pressure is measured with the two hose bars in the center of the chamber. The static pressure is measured with the hose barb closest to the front plate and the pressure will be positive for the airflow into the chamber. Pressure drop across the nozzles is measured with a differential pressure transducer (setra model 264; +/-0.25%, +/-0.4%, 1% FS accuracy; 0-10PSI). The pressure applied to the test object is important to know since air flow is relative to the applied pressure differential. This pressure is usually measured in Inches of Water column or "wc. The overall pressure drops, channel wall temperature, and power to each channel are recorded using a data acquisition (DAQ) unit (34972A, Agilent).

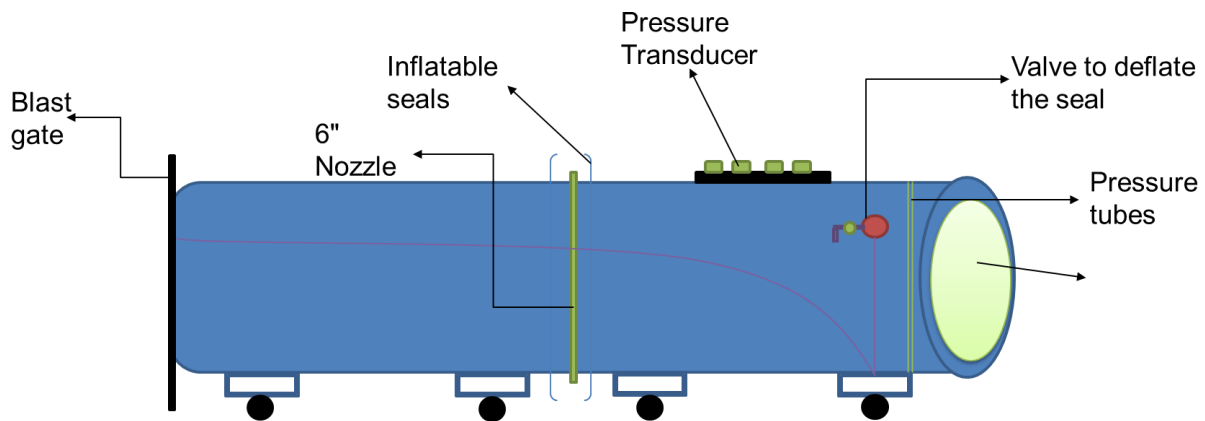


Fig 11 – Schematic image of Air flow bench

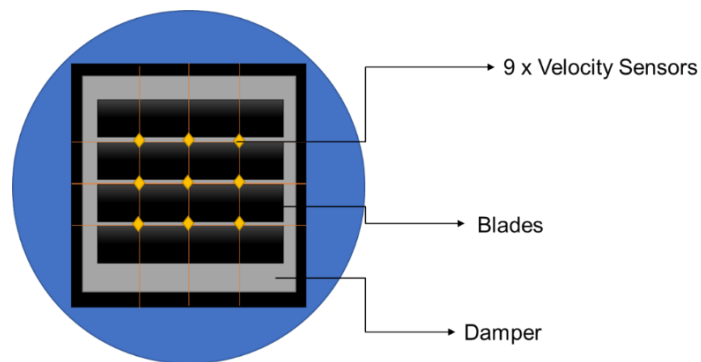


Fig 12 – Schematic image of front section of Air flow bench with Damper



The photograph of the custom built 4m long closed cuboid setup as shown in fig 13 is made with velocity sensors attached at the end of the cuboid setup to ensure neglecting the turbulence formed. A 3x3 mesh type is made with the help of strings and the velocity sensors are attached to it as shown in fig 15. In which these velocity sensors are already calibrated. Then the setup is run at different frequencies to plot a graph. With the help of the graph, a slope is taken out to get gain and offset values. Then, the pressure reading from the nozzle and the flow sensor are compared and calibrated by changing the gain and offset values.



Fig 13 – Image of Air Flow Bench

Once the setup is calibrated, a 24\*24" damper as shown in fig 6 single side opening blades is attached to the airflow bench to determine the pressure within the chamber and the atmospheric pressure. This damper is then run at four different angles, 30, 50, and 80 degrees, at different air flow frequencies such as 20hz, 30hz, 40hz to plot a graph. Subsequently, another damper with 4 crossflow opening blades as shown in fig 14 is attached to the airflow bench, and the same procedure is repeated.



Fig 14 – Image of Front section of Air flow bench

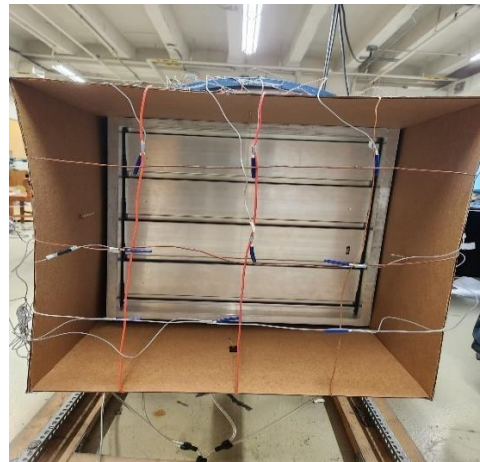


Fig 15 – Image of Air flow bench with Flow sensors

Then, the same experiment is repeated with 1.5m cuboid setup extended from the damper where the atmospheric pressure is measured at a desired distance from the damper to make a study.

**Damper Characterization Graph:**

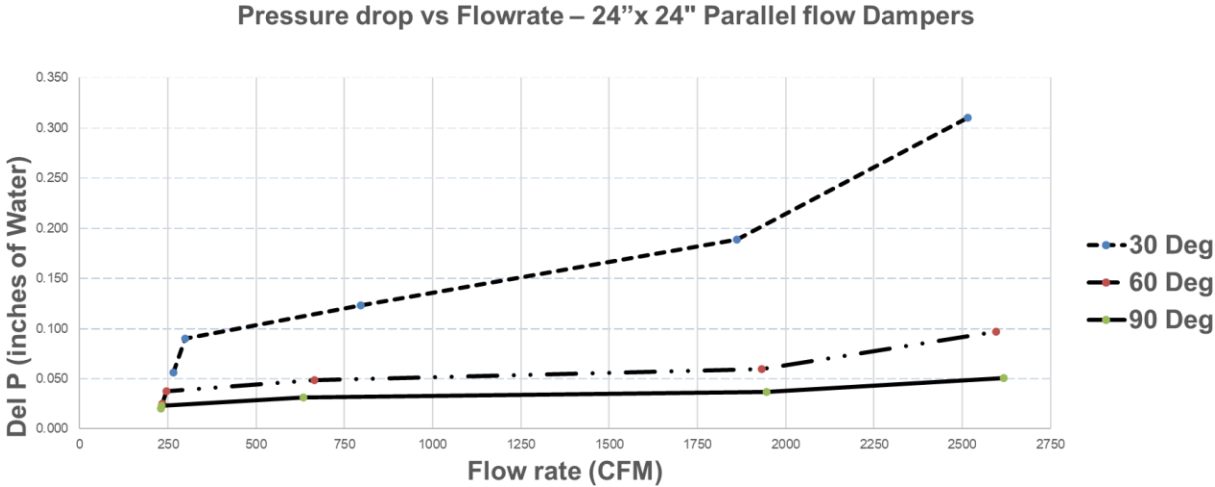


Fig 16- Plot for Pressure drop vs Flow rate

The shape of the Del P vs flow rate graph can reveal important information about the system or component being studied. For example, a flat or nearly flat curve may indicate that the system has low resistance to flow, while a steep or sharply rising curve may suggest that the system is becoming increasingly restricted as flow increases.

In addition, it helps analyze the performance of fluid flow systems, Del P vs flow rate graphs can also be used to optimize the design and operation of such systems. By studying the graph and identifying the point at which maximum flow is achieved with the least amount of pressure drop.

## Chapter 5

### CFD MODELING

The Aztec ASC 5 model from Mestex is considered for the CFD modelling. Numerical modeling analysis is done using 6SigmaRoom CFD tool by Future Facilities. 6Sigma Room is a commercial computational fluid dynamics (CFD) software tool designed specifically for the analysis of indoor air quality and thermal comfort in buildings.

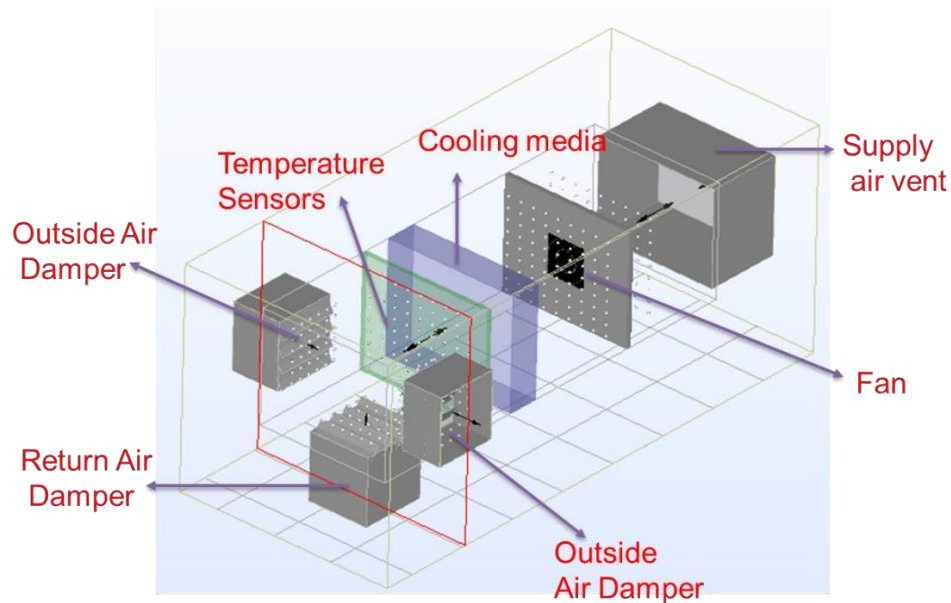


Fig 17 – CFD model for Air handling unit

#### **Model Specification:**

##### Geometrical Specification

AHU Chamber size – 42.5 \* 52 \* 152 inches

Return air vent size – 24 \* 24 inches

Outdoor air vent size – 24 \* 24 inches

Damper size – 0.5 \* 24 \* 24 inches

##### **Fan Specification**

Fan Diameter – 15 inches

Fan Flow rate – 2000 CFM

Number of Fans – 1

### Evaporative Pad Specification

Number of cooling pads – 1

Pad thickness – 12 inches

Pad dimension – 42.5 \* 52 inches

Note: Mixing chamber dimensions are replicated from Aztec ASC 5 unit

### Boundary Conditions:

1. Outside Air Temperature - 37F
2. Return Air Temperature - 117F
3. Target Mixed Air Temperature - 80F
4. k-ε Turbulence model
5. No. of Fans - 1
6. Total Flow Rate – 2000 CFM
7. Total Cell Count – 0.8 million

### Adiabatic mixing:

Adiabatic mixing is a psychrometric process where we mix two different air streams to obtain a third mixed air stream. The conditions of the resulting mixture can be obtained from the mass and energy balance [25-28].

$$\text{Energy Balance: } m_1h_1+m_2h_2=m_3h_3$$

$$\text{Mass Balance: } m_1+m_2=m_3$$



Fig 18 - Adiabatic mixing schematic with process line on the psychrometric chart [25]

In this study, we have chosen two streams at temperature of 37-degree Fahrenheit and 117-degree Fahrenheit at a relative humidity of 50% for both streams. Outdoor air temperature was set at 37F because the lowest average temperature in a year in Dallas-Fort Worth area was 37F and the return air temperature was chosen as 117F because a typical class A4 has return air temperature up to 117F. So, these extreme cases were considered to study the mixing phenomenon.

The first and second air stream points were plotted and connected by a straight line to determine the desired temperature of the mixed air, which was set at 80°F. All other conditions were derived from the psychrometric chart. This graphing allows us to determine the proportion of each air stream, or the OA/RA ratio. 40 percent of the whole volume was determined to be RA.

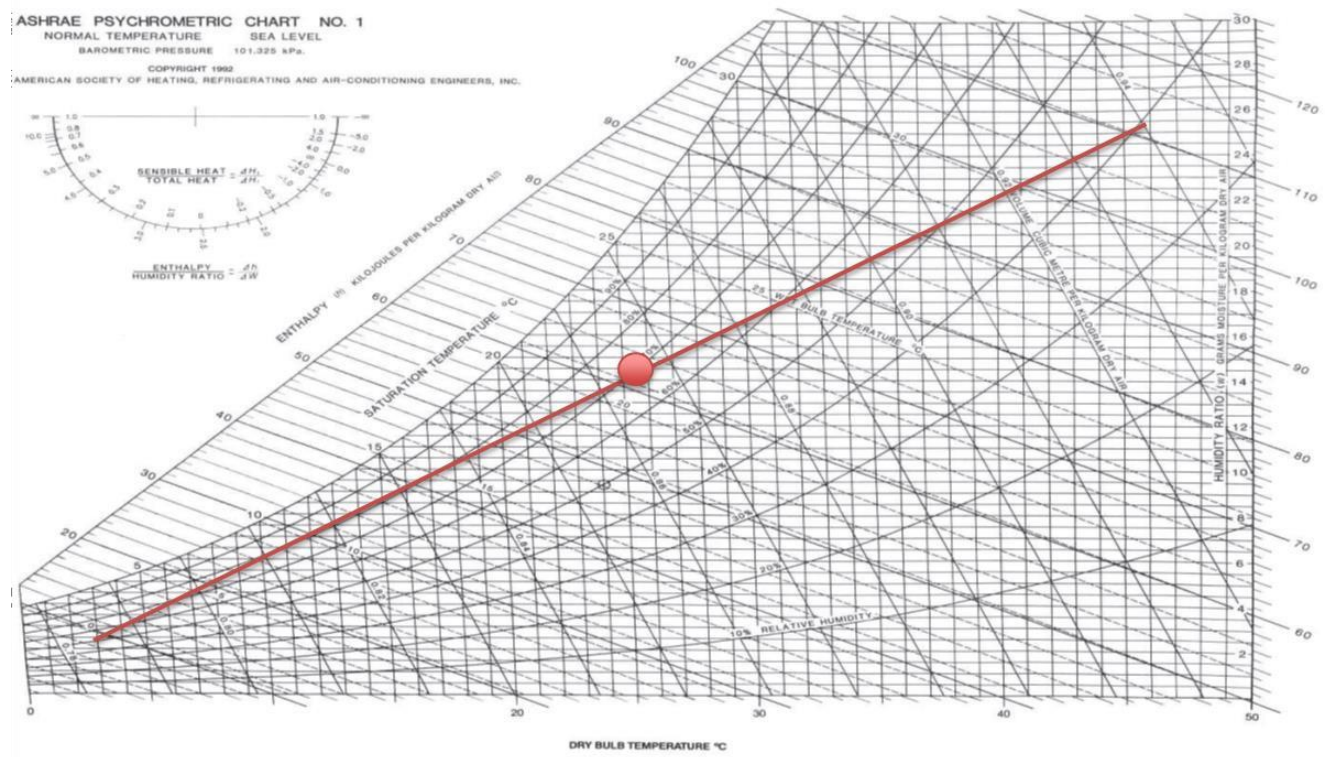


Fig 19 - Adiabatic mixing of OA and RA on psychrometric chart

### Mixing Effectiveness

Mixing of two streams can be quantified using mixing effectiveness such as range effectiveness[9].

$$\text{Mixing Effectiveness} = \left[ 1 - \frac{(T_{max} - T_{min})}{(T_{RA} - T_{OA})} \right] * 100\%$$

Where,

T max- Maximum Temperature in the plane of measurement

T min- Minimum Temperature in the plane of measurement

T RA- Return Air Temperature

T OA- Outdoor Air Temperature

### Grid Sensitivity Analysis:

Grid sensitivity analysis is carried out to make the model accuracy independent of the mesh size. By carrying out grid sensitivity analysis we can find the minimum number of grids that is needed for the model, increasing the grid count after which is irrelevant to the accuracy of the model, and it just increases the computation power [30-46]. Grid sensitivity for this study was carried out on dampers since most of the model is open and plain. From the literature review we can say that grid sensitivity analysis is an essential step in numerical simulations, ensuring the accuracy and reliability of the results. By systematically investigating the impact of grid changes, engineers and scientists can make informed decisions regarding the appropriate grid resolution for their specific applications [47-55].

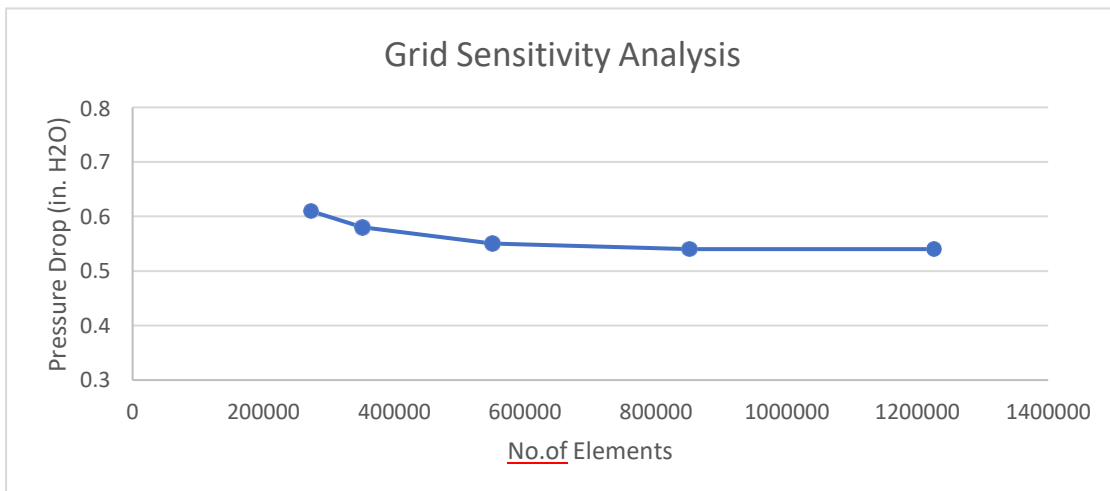


Fig 20 – Plot for Grid Sensitivity Analysis

## Chapter 6

### Results and Discussion

The mixing of air streams plays a vital role in determining the efficiency of the evaporative cooling media. Usually, poor efficiency leads to higher pumping power for the evaporative media. The objective of this article is to analyze the effect of different damper combinations (parallel/opposed blade), for different angles such as 30°, 50°, and 80°. This is done by a commercially available software, 6sigmaroom.

#### Damper Combination

Case	Return Air	Outside Air	Outside Air	Vent Angle
1	Parallel	Parallel	Parallel	30
				50
				80
2	Opposed	Opposed	Opposed	30
				50
				80
3	Parallel	Opposed	Opposed	30
				50
				80
4	Parallel	Parallel	Opposed	30
				50
				80
5	Opposed	Opposed	Parallel	30
				50
				80
6	Parallel	Opposed	Parallel	30
				50
				80

Fig 21 – Table for Different Damper Combination

So, there are overall 6 cases with the combination of return air, outside air and vent angles which makes an overall combination of 54.

### Mixing Effectiveness and Pressure drop observations:

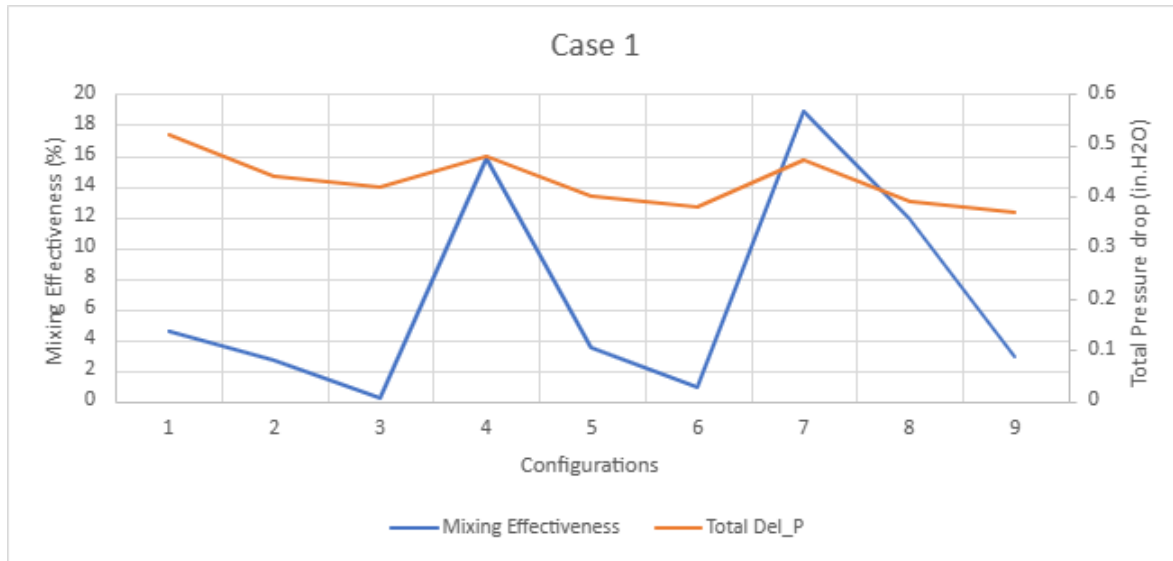


Fig 22 – Plot for Mixing Effectiveness and Total pressure drop vs different configurations for case 1

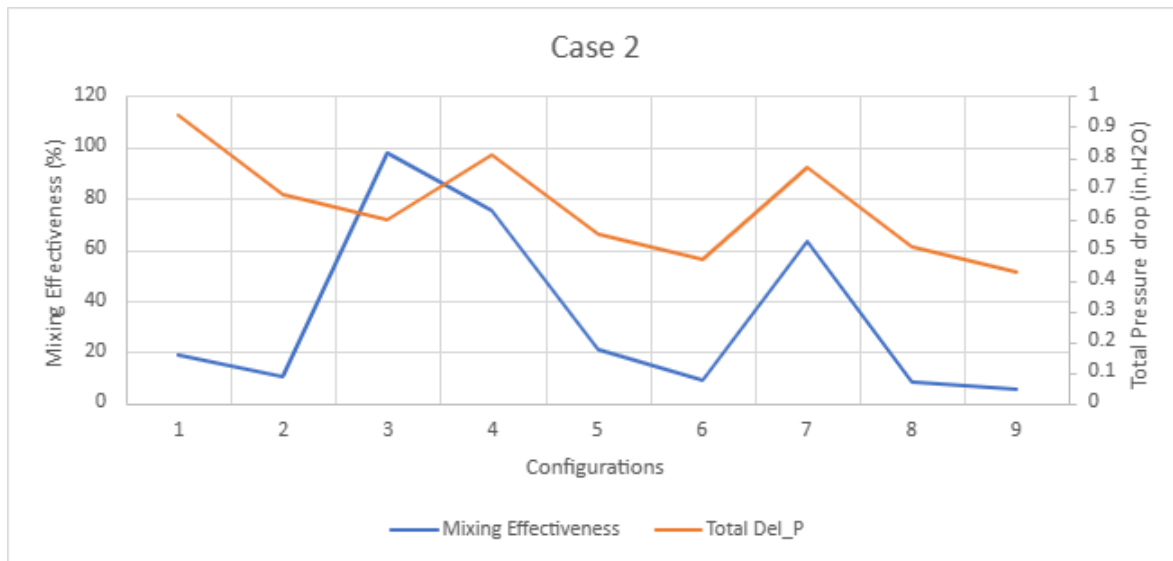


Fig 23 – Plot for Mixing Effectiveness and Total pressure drop vs different configurations for case 2



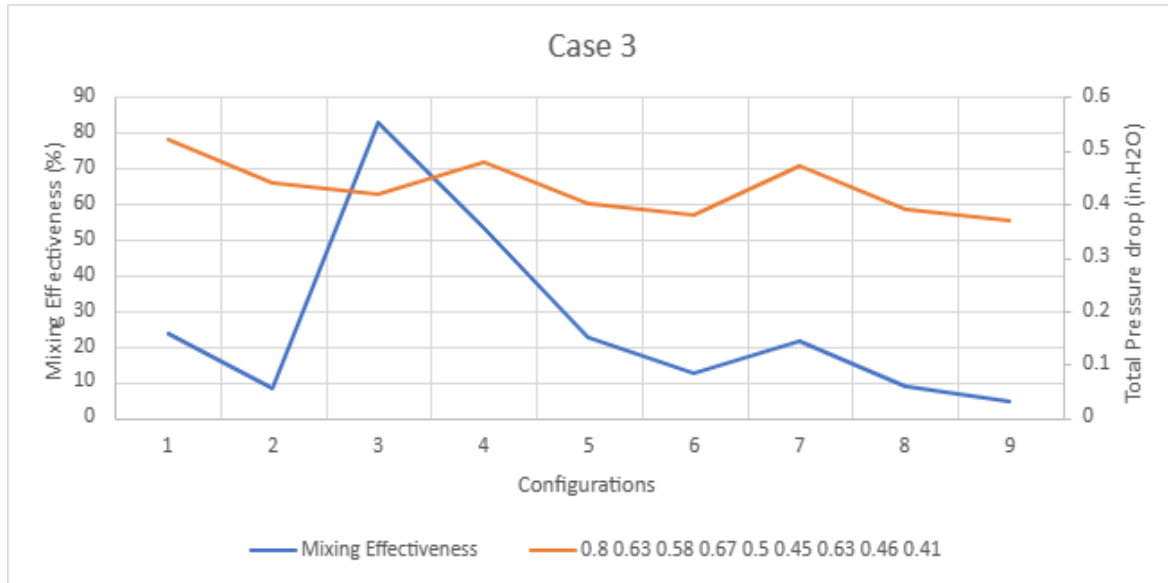


Fig 24 – Plot for Mixing Effectiveness and Total pressure drop vs different configurations for case 3

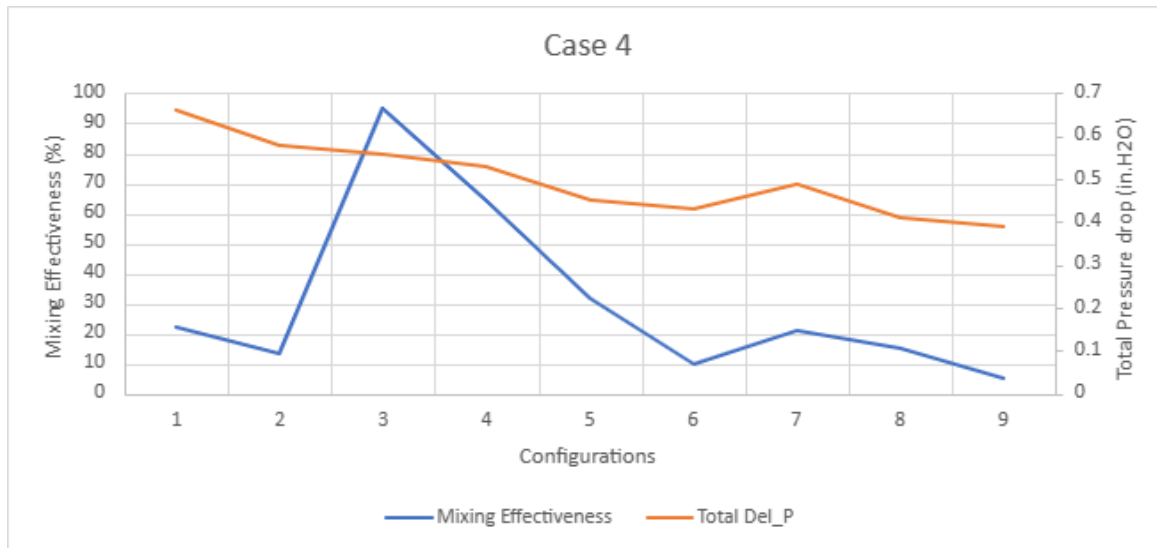


Fig 25 – Plot for Mixing Effectiveness and Total pressure drop vs different configurations for case 4

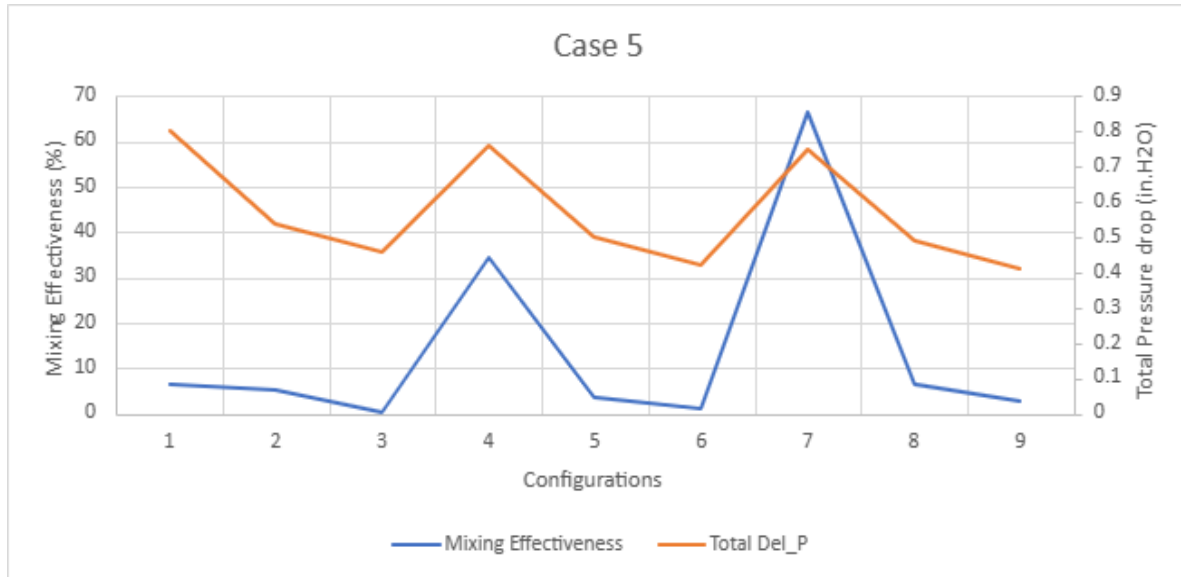


Fig 26 – Plot for Mixing Effectiveness and Total pressure drop vs different configurations for case 5

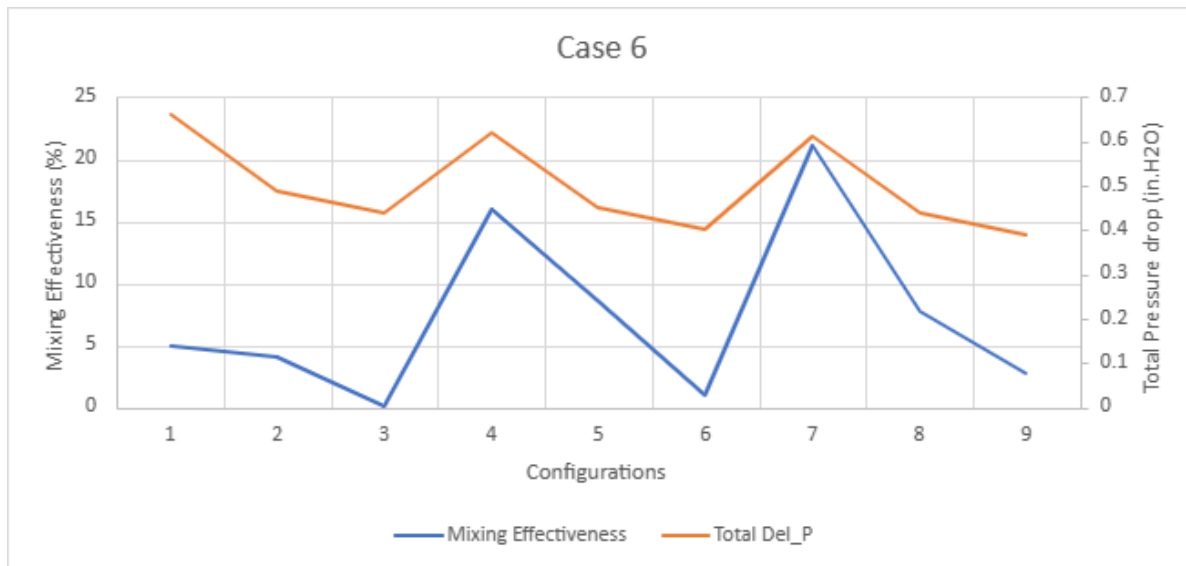


Fig 27 – Plot for Mixing Effectiveness and Total pressure drop vs different configurations for case 6

### Mixing Effectiveness Comparison:

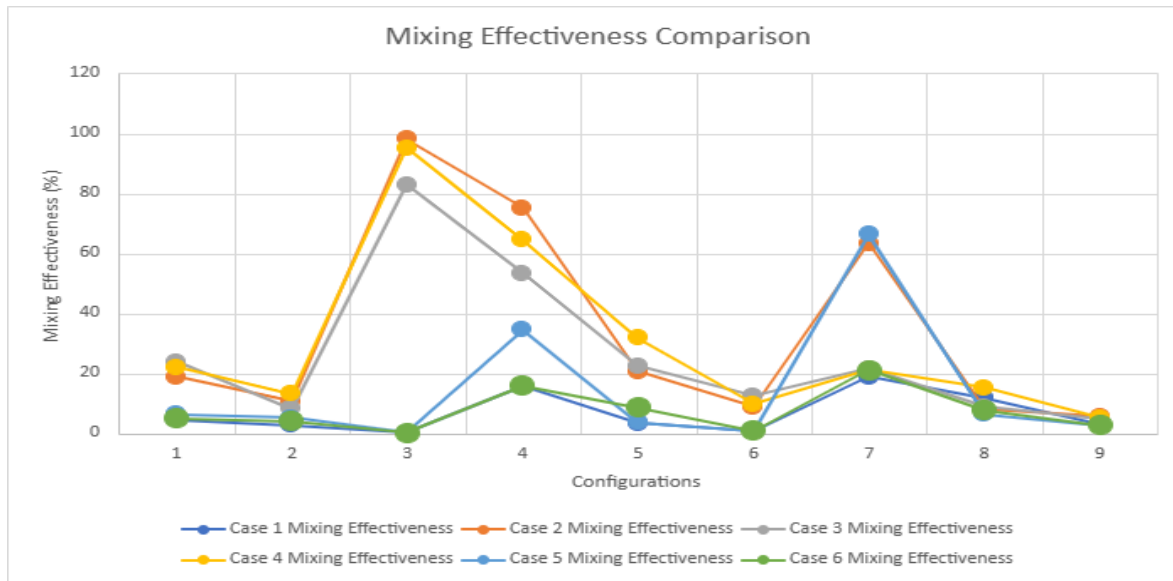


Fig 28 – Plot for Mixing Effectiveness Comparison

According to the graph, it is evident that case 2 exhibits the highest air mixing effectiveness compared to the other cases. This conclusion is supported by the damper combination table, where case 2 utilizes opposed return air damper and opposed outside air damper configurations. This configuration suggests that using opposed dampers for both return and outside air contributes to a higher percentage of air mixing effectiveness. On the other hand, in case 1, both the outside air damper and return air damper are parallel dampers, which results in the lowest air mixing effectiveness among the different cases.

### Pressure Drop Comparison:

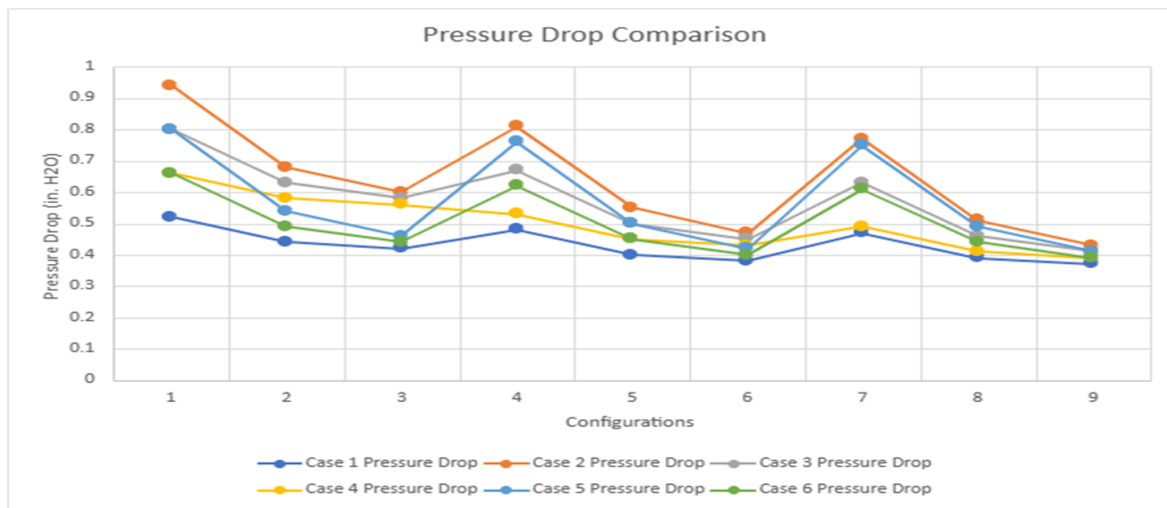


Fig 29 – Plot for Pressure drop Comparison

From the above graph, we can say that the pressure drops for case 4 with respect to the configuration is linear and less when compared to case 2. As we know less pressure drop and flow rate value will less to low pumping power. So, higher the pressure drop value, higher will be the pumping power and vice versa.

**Temperature Contours:**

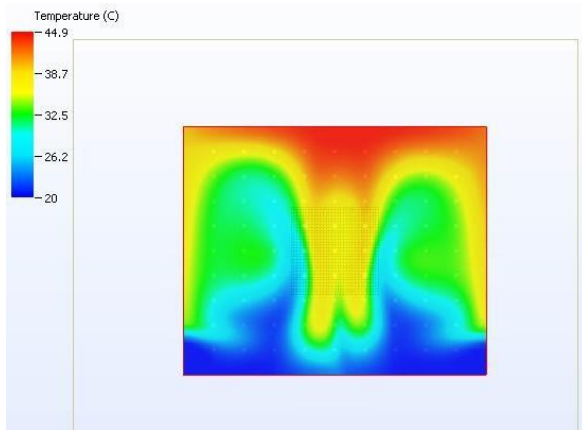


Fig 30 – Temperature Contour for Case 2

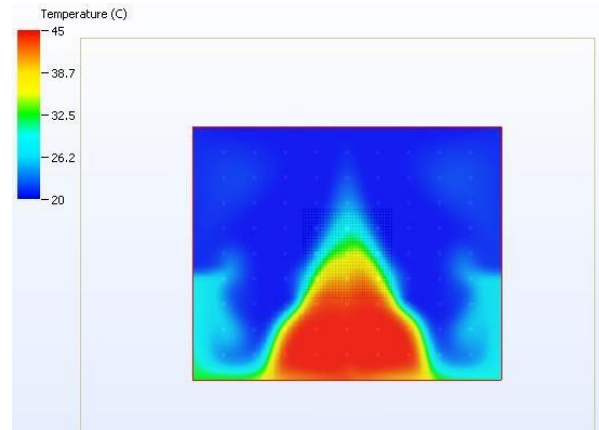


Fig 31 – Temperature Contour for Case 3

The figures provided, Fig 30 and Fig 31, depict temperature contours for the cases with the highest and lowest air mixing effectiveness, respectively. The image on the left represents a scenario where maximum air mixing effectiveness of 98% is achieved, while the image on the right corresponds to the case with the lowest air mixing effectiveness of 1%. It is important to note that in this study, the values have been normalized to facilitate comparison and analysis.

**Velocity Vectors:**

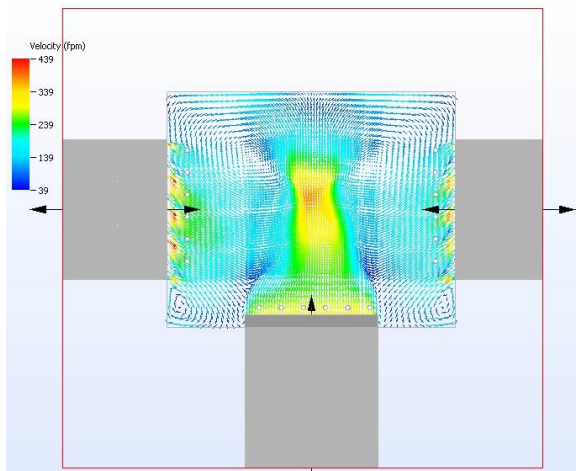


Fig 32 – Velocity Vectors for Case 2

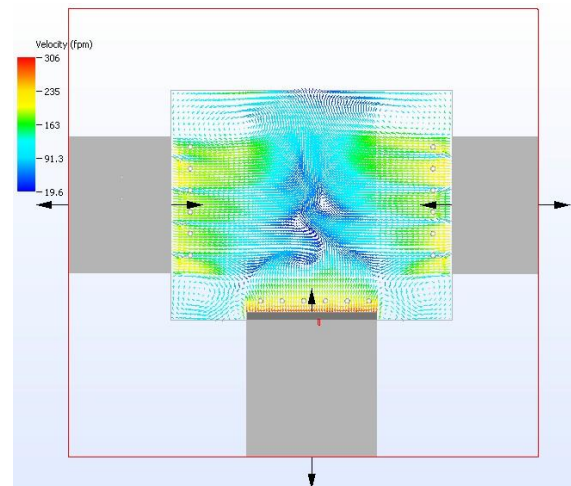


Fig 33 – Velocity Vectors for Case 3

Figures 32 and 33 display Velocity Vectors for the cases with maximum and minimum air mixing effectiveness, respectively. In the image on the left (Fig 32), it is visually apparent that the air is well-mixed, resulting in reduced thermal stratification. Conversely, the image on the right (Fig 33) illustrates poor air mixing, leading to inadequate air mixing effectiveness and significant thermal stratification. By analyzing the velocity vectors, one can observe the flow patterns and understand the impact they have on air mixing. The clear distinction between the two images highlights the importance of effective air mixing for minimizing thermal stratification within the space.

## Chapter 7

### Conclusion

The objective of this study was to address the issue of thermal stratification in air handlers that often occurs under varying operating conditions, and to improve the air mixing effectiveness to reduce the pumping power required for direct evaporative cooling using a cooling media. The findings of the study clearly demonstrate that using opposed blade dampers is an effective approach to achieving good air mixing, as compared to parallel blade dampers. In conclusion, for the Aztec 5 model, it can be concluded that the most effective arrangement of Return air damper blades is through the implementation of opposed blade dampers, which have the potential to significantly reduce thermal stratification and improve cooling efficiency. These results have significant practical implications, as they can guide the design and operation of air handling systems, ultimately leading to energy savings and enhanced performance.

In future, including details about the shape of the opposed blade is important because it can affect the level of turbulence and mixing that occurs. By considering the shape of the blades, one can imagine that it may influence the flow of the fluid, potentially leading to an increase in turbulence and ultimately resulting in a greater level of mixing. Therefore, it is crucial to consider the blade's shape when analyzing mixing processes. And, vertical dampers are often preferred for their ability to provide more accurate airflow control, especially in systems where it is crucial to maintain a certain pressure.

## Reference:

1. Modi, Himanshu, Uschas Chowdhury, and Dereje Agonafer. "Impact of Improved Ducting and Chassis Re-design for Air-Cooled Servers in a Data Center." In 2022 21st IEEE Intersociety Conference on Thermal and Thermomechanical Phenomena in Electronic Systems (iTherm), pp. 1-8. IEEE, 2022.
2. Modi, Himanshu, Pardeep Shahi, Akiilesh Sivakumar, Satyam Saini, Pratik Bansode, Vibin Shalom, Amrutha Valli Rachakonda, Gautam Gupta, and Dereje Agonafer. "Transient CFD Analysis of Dynamic Liquid-Cooling Implementation at Rack Level." In International Electronic Packaging Technical Conference and Exhibition, vol. 86557, p. V001T01A012. American Society of Mechanical Engineers, 2022.
3. Modi, Himanshu, Pardeep Shahi, Lochan Sai Reddy Chinthaparthi, Gautam Gupta, Pratik Bansode, Vibin Shalom Simon, and Dereje Agonafer. "Experimental Investigation of the Impact of Improved Ducting and Chassis Re-Design of a Hybrid-Cooled Server." In International Electronic Packaging Technical Conference and Exhibition, vol. 86557, p. V001T01A019. American Society of Mechanical Engineers, 2022.
4. Heydari, Ali, Pardeep Shahi, Vahideh Radmard, Bahareh Eslami, Uschas Chowdhury, Chandraprakash Hinge, Lochan Sai Reddy Cinthaparthi et al. "A Control Strategy for Minimizing Temperature Fluctuations in High Power Liquid to Liquid CDUs Operated at Very Low Heat Loads." In International Electronic Packaging Technical Conference and Exhibition, vol. 86557, p. V001T01A011. American Society of Mechanical Engineers, 2022.
5. Shalom Simon, Vibin, Lochan Sai Reddy, Pardeep Shahi, Amrutha Valli, Satyam Saini, Himanshu Modi, Pratik Bansode, and Dereje Agonafer. "CFD Analysis of Heat Capture Ratio in a Hybrid Cooled Server." In International Electronic Packaging Technical Conference and Exhibition, vol. 86557, p. V001T01A013. American Society of Mechanical Engineers, 2022.
6. Murthy, Prajwal, Gautam Gupta, Joseph Herring, Jacob Lamotte-Dawaghreh, Krishna Bhavana Sivaraju, Pratik Bansode, Himanshu Modi, Dereje Agonafer, Poornima Mynampati, and Mike Sweeney. "CFD Simulation-Based Comparative Study of Forced Convection Single-Phase Liquid Immersion Cooling for a High-Powered Server." In International Electronic Packaging Technical Conference and Exhibition, vol. 86557, p. V001T01A006. American Society of Mechanical Engineers, 2022.
7. Shalom Simon, Vibin, Himanshu Modi, Krishna Bhavana Sivaraju, Pratik Bansode, Satyam Saini, Pardeep Shahi, Saket Karajgikar, Veerendra Mulay, and Dereje Agonafer. "Feasibility Study of Rear Door Heat Exchanger for a High Capacity Data Center." In International Electronic Packaging Technical Conference and Exhibition, vol. 86557, p. V001T01A018. American Society of Mechanical Engineers, 2022.
8. Modi, Himanshu. "Computational Study of Air-Cooled Servers with Improved Ducting and Chassis Re-design." PhD diss., The University of Texas at Arlington, 2020.

9. Shahi, Pardeep, Satyam Saini, Pratik Bansode, and Dereje Agonafer. "A comparative study of energy savings in a liquid-cooled server by dynamic control of coolant flow rate at server level." *IEEE Transactions on Components, Packaging and Manufacturing Technology* 11, no. 4 (2021): 616-624.
10. Shahi, Pardeep, Sarthak Agarwal, Satyam Saini, Amirreza Niazmand, Pratik Bansode, and Dereje Agonafer. "CFD analysis on liquid cooled cold plate using copper nanoparticles." In *International Electronic Packaging Technical Conference and Exhibition*, vol. 84041, p. V001T08A007. American Society of Mechanical Engineers, 2020.
11. Shahi, Pardeep, Amith Mathew, Satyam Saini, Pratik Bansode, Rajesh Kasukurthy, and Dereje Agonafer. "Assessment of Reliability Enhancement in High-Power CPUs and GPUs Using Dynamic Direct-to-Chip Liquid Cooling." *Journal of Enhanced Heat Transfer* 29, no. 8 (2022).
12. Shahi, Pardeep, Apruv Pravin Deshmukh, Hardik Yashwant Hurnekar, Satyam Saini, Pratik Bansode, Rajesh Kasukurthy, and Dereje Agonafer. "Design, Development, and Characterization of a Flow Control Device for Dynamic Cooling of Liquid-Cooled Servers." *Journal of Electronic Packaging* 144, no. 4 (2022).
13. Shahi, Pardeep, Apurv Deshmukh, Hardik Yashwant Hurnekar, Satyam Saini, Pratik Bansode, and Dereje Agonafer. "Numerical Investigation on Effect of Target Coolant Delivery in Liquid-Cooled Microchannel Heat Sinks." *Journal of Enhanced Heat Transfer* 30, no. 1 (2023).
14. Shahi, Pardeep, Hardik Yashwant Hurnekar, Apurv Deshmukh, Satyam Saini, Pratik Bansode, Rajesh Kasukurthy, and Dereje Agonafer. "Assessment of Pump Power Savings at Rack level for Dynamic Direct-to-Chip Liquid Cooling Using a Novel Flow Control Device." *Journal of Enhanced Heat Transfer* 30, no. 1 (2023).
15. Heydari, Ali, Pardeep Shahi, Vahideh Radmard, Bahareh Eslami, Uschas Chowdhury, Satyam Saini, Pratik Bansode, Harold Miyamura, Dereje Agonafer, and Jeremy Rodriguez. "Liquid to Liquid Cooling for High Heat Density Liquid Cooled Data Centers." In *International Electronic Packaging Technical Conference and Exhibition*, vol. 86557, p. V001T01A007. American Society of Mechanical Engineers, 2022.
16. Shahi, Pardeep, Satyam Saini, Pratik Bansode, Rajesh Kasukurthy, and Dereje Agonafer. "Experimental Study Demonstrating Pumping Power Savings at Rack Level Using Dynamic Cooling." *Journal of Enhanced Heat Transfer* 29, no. 6 (2022).
17. <https://www.techtargget.com/searchdatacenter/tip/How-much-energy-do-data-centers-consume>
18. <https://uptimeinstitute.com/resources/asset/2021-data-center-industry-survey>
19. ASHRAE specifications per class, <http://www.anandtech.com/show/7723/free-cooling-the-server-side-of-the-story/3>.
20. ASHRAE TC9.9 - Data Center Power Equipment Thermal Guidelines and Best Practices [https://tc0909.ashraetcs.org/documents/ASHRAE\\_TC0909\\_Power\\_White\\_Paper\\_22\\_June\\_2016\\_REVISED.pdf](https://tc0909.ashraetcs.org/documents/ASHRAE_TC0909_Power_White_Paper_22_June_2016_REVISED.pdf)



21. N. Shah, "CFD Analysis of Direct Evaporative Cooling Zone of Air-side Economizer for Containerized Data Center," May 2012.
22. Thesis Dissertation (MSME- PAVAN VIJAYKUMAR KAULGUD,UTA)
23. Thesis Dissertation (MSME- AVINASH KUMAR RAY, UTA )
24. The Different Technologies for Cooling Data Centers – White paper # 59 by Tony Evans
25. Adiabatic mixing  
<https://nptel.ac.in/courses/112105129/pdf/R&AC%20Lecture%2028.pdf>
26. Thesis Dissertation (MSME- ANTO JOSEPH BARIGALA CHARLES PAULRAJ, UTA)
27. P. Kaulgud, A. Siddarth, V. S. Simon, and D. Agonafer, "Characterization of parallel and opposed control dampers to observe the effect on thermal mixing of air streams in an air-cooling unit," 2022.
28. Shalom Simon, V, Modi, H, Sivaraju, KB, Bansode, P, Saini, S, Shahi, P, Karajgikar, S, Mulay, V, & Agonafer, D. "Feasibility Study of Rear Door Heat Exchanger for a High-Capacity Data Center." 2022.
29. V. S. Simon, "Methodology to Develop Artificial Neural Network Based Control Strategies for Multiple Air-Cooling Units in a Raised Floor Data Center." Order No. 28208251, The University of Texas at Arlington, United States -- Texas, 2019.
30. Heydari, Ali, Pardeep Shahi, Vahideh Radmard, Bahareh Eslami, Uschas Chowdhury, Akiilessh Sivakumar, Akshay Lakshminarayana et al. "Experimental Study of Transient Hydraulic Characteristics for Liquid Cooled Data Center Deployment." In International Electronic Packaging Technical Conference and Exhibition, vol. 86557, p. V001T01A009. American Society of Mechanical Engineers, 2022.
31. Shahi, Pardeep. "Experimental Analysis of PCM based Thermal Storage System for Solar Power Plant." PhD diss., MS thesis, Indian Institute of Technology-Mumbai, 2016.
32. Thirunavakkarasu, Gautham, Satyam Saini, Jimil Shah, and Dereje Agonafer. "Air flow pattern and path flow simulation of airborne particulate contaminants in a high-density data center utilizing airside economization." In International Electronic Packaging Technical Conference and Exhibition, vol. 51920, p. V001T02A011. American Society of Mechanical Engineers, 2018.
33. Shah, Jimil M., Roshan Anand, Satyam Saini, Rawhan Cyriac, Dereje Agonafer, Prabjit Singh, and Mike Kaler. "Development of a technique to measure deliquescent relative humidity of particulate contaminants and determination of the operating relative humidity of a data center." In International Electronic Packaging Technical Conference and Exhibition, vol. 59322, p. V001T02A016. American Society of Mechanical Engineers, 2019.
34. Saini, Satyam, Aryan Gupta, Aman Jyoti Mehta, and Sumit Pramanik. "Rice husk-extracted silica reinforced graphite/aluminium matrix hybrid composite." *Journal of Thermal Analysis and Calorimetry* (2020): 1-10.

35. Shah, Jimil M., Roshan Anand, Prabjit Singh, Satyam Saini, Rawhan Cyriac, Dereje Agonafer, and Mike Kaler. "Development of a Precise and Cost-Effective Technique to Measure Deliquescent Relative Humidity of Particulate Contaminants and Determination of the Operating Relative Humidity of a Data Center Utilizing Airside Economization." *Journal of Electronic Packaging* 142, no. 4 (2020).
36. Niazmand, Amirreza, Prajwal Murthy, Satyam Saini, Pardeep Shahi, Pratik Bansode, and Dereje Agonafer. "Numerical analysis of oil immersion cooling of a server using mineral oil and Al<sub>2</sub>O<sub>3</sub> nanofluid." In *International Electronic Packaging Technical Conference and Exhibition*, vol. 84041, p. V001T08A009. American Society of Mechanical Engineers, 2020.
37. Saini, Satyam, Pardeep Shahi, Pratik Bansode, Ashwin Siddarth, and Dereje Agonafer. "CFD investigation of dispersion of airborne particulate contaminants in a raised floor data center." In *2020 36th Semiconductor Thermal Measurement, Modeling & Management Symposium (SEMI-THERM)*, pp. 39-47. IEEE, 2020.
38. Niazmand, Amirreza, Tushar Chauhan, Satyam Saini, Pardeep Shahi, Pratik Vithoba Bansode, and Dereje Agonafer. "CFD simulation of two-phase immersion cooling using FC-72 dielectric fluid." In *International Electronic Packaging Technical Conference and Exhibition*, vol. 84041, p. V001T07A009. American Society of Mechanical Engineers, 2020.
39. Saini, Satyam. "Airflow path and flow pattern analysis of sub-micron particulate contaminants in a data center with hot aisle containment system utilizing direct air cooling." PhD diss., The University of Texas at Arlington, 2018.
40. Saini, Satyam, Jimil M. Shah, Pardeep Shahi, Pratik Bansode, Dereje Agonafer, Prabjit Singh, Roger Schmidt, and Mike Kaler. "Effects of Gaseous and Particulate Contaminants on Information Technology Equipment Reliability—A Review." *Journal of Electronic Packaging* 144, no. 3 (2022).
41. Saini, Satyam, Kaustubh K. Adsul, Pardeep Shahi, Amirreza Niazmand, Pratik Bansode, and Dereje Agonafer. "CFD Modeling of the Distribution of Airborne Particulate Contaminants Inside Data Center Hardware." In *International Electronic Packaging Technical Conference and Exhibition*, vol. 84041, p. V001T08A005. American Society of Mechanical Engineers, 2020.
42. Gandhi, Dhruvkumar, Uschas Chowdhury, Tushar Chauhan, Pratik Bansode, Satyam Saini, Jimil M. Shah, and Dereje Agonafer. "Computational analysis for thermal optimization of server for single phase immersion cooling." In *International Electronic Packaging Technical Conference and Exhibition*, vol. 59322, p. V001T02A013. American Society of Mechanical Engineers, 2019.
43. Saini, Satyam, Tushar Wagh, Pratik Bansode, Pardeep Shahi, Joseph Herring, Jacob Lamotte-Dawaghreh, Jimil M. Shah, and Dereje Agonafer. "A Numerical Study on Multi-Objective Design Optimization of Heat Sinks for Forced and Natural Convection Cooling of Immersion-Cooled Servers." *Journal of Enhanced Heat Transfer* 29, no. 8 (2022).

44. Shah, Jimil M., Chinmay Bhatt, Pranavi Rachamreddy, Ravya Dandamudi, Satyam Saini, and Dereje Agonafer. "Computational form factor study of a 3rd generation open compute server for single-phase immersion cooling." In International Electronic Packaging Technical Conference and Exhibition, vol. 59322, p. V001T02A017. American Society of Mechanical Engineers, 2019.
45. Shah, Jimil M., Keerthivasan Padmanaban, Hrishabh Singh, Surya Duraisamy Asokan, Satyam Saini, and Dereje Agonafer. "Evaluating the Reliability of Passive Server Components for Single-Phase Immersion Cooling." *Journal of Electronic Packaging* 144, no. 2 (2022).
46. Saini, Satyam, Pardeep Shahi, Pratik Bansode, Jimil M. Shah, and Dereje Agonafer. "Simplified and Detailed Analysis of Data Center Particulate Contamination at Server and Room Level Using Computational Fluid Dynamics." *Journal of Electronic Packaging* 144, no. 2 (2022): 024501.
47. Misrak, A., Chauhan, T., Rajmane, P., Bhandari, R., and Agonafer, D. (November 8, 2019). "Impact of Aging on Mechanical Properties of Thermally Conductive Gap Fillers." *ASME. J. Electron. Packag.* March 2020; 142(1): 011011. <https://doi.org/10.1115/1.4045157>
48. T. Chauhan, A. Misrak, R. Bhandari, P. Rajmane, A. S. M. R. Chowdhury, K. B. Sivaraju, M. Abdulhasansari, and D. Agonafer, "Impact of thermal aging and cycling on reliability of thermal interface materials," in *Proceedings of SMTA International*. Rosemont, IL, USA: SMTA, 2019, pp. 118–123.
49. Rajmane P, Mirza F, Khan H, Agonafer D. "Chip Package Interaction Study to Analyze the Mechanical Integrity of a 3-D TSV Package," *ASME. International Electronic Packaging Technical Conference and Exhibition, Volume 2: Advanced Electronics and Photonics, Packaging Materials and Processing; Advanced Electronics and Photonics: Packaging, Interconnect and Reliability; Fundamentals of Thermal and Fluid Transport in Nano, Micro, and Mini Scales ()*: V002T02A009. doi:10.1115/IPACK2015-48811.
50. U. Rahangdale, P. Rajmane, "Structural integrity optimization of 3D TSV package by analyzing crack behavior at TSV and BEOL," 2017 28th Annual SEMI Advanced Semiconductor Manufacturing Conference (ASMC), Saratoga Springs, NY, USA, 2017, pp. 201-208. doi: 10.1109/ASMC.2017.7969230
51. U. Rahangdale et al., "Damage progression study of 3D TSV package during reflow, thermal shocks and thermal cycling," 2017 16th IEEE Intersociety Conference on Thermal and Thermomechanical Phenomena in Electronic Systems (ITherm), Orlando, FL, 2017, pp. 1119-1125, doi: 10.1109/ITHERM.2017.7992614.
52. Rahangdale, Unique, Rajmane, Pavan, Misrak, Abel, and Agonafer, Dereje. "Reliability Analysis of Ultra-Low-K Large-Die Package and Wire Bond Chip Package on Varying Structural Parameter Under
53. Thermal Loading." *Proceedings of the ASME 2017 International Technical Conference and Exhibition on Packaging and Integration of Electronic and Photonic Microsystems collocated with the ASME 2017 Conference on Information Storage and Processing*

Systems. ASME 2017 International Technical Conference and Exhibition on Packaging and Integration of Electronic and Photonic Microsystems. San Francisco, California, USA. August 29–September 1, 2017. V001T01A020. ASME.

54. P. Rajmane, "MULTI-PHYSICS DESIGN OPTIMIZATION OF 2D AND ADVANCED HETEROGENOUS 3D INTEGRATED CIRCUITS," in University of Texas at Arlington, Arlington, Texas, 2018.
55. Chinthaparthi, Lochan Sai Reddy. 2021. Accelerated performance degradation of single-phase cold plates for direct-to-chip liquid cooled data centers. Ph.D. diss., The University of Texas at Arlington,  
<https://login.ezproxy.uta.edu/login?url=https://www.proquest.com/dissertations-theses/accelerated-performance-degradation-single-phase/docview/2640031815/se-2>  
(accessed May 16, 2023).